CuInSe2 Quantum Dot Solar Cells with High Open-Circuit Voltage

ARTICLE *in* JOURNAL OF PHYSICAL CHEMISTRY LETTERS · JUNE 2013

Impact Factor: 7.46 · DOI: 10.1021/jz4010015

8 AUTHORS, INCLUDING:

Matthew Panthani
University of Chicago
34 PUBLICATIONS **1,770** CITATIONS
SEE PROFILE

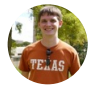

C. Jackson Stolle
University of Texas at Austin
12 PUBLICATIONS **235** CITATIONS
SEE PROFILE

Taylor Harvey
University of Texas at Austin
11 PUBLICATIONS **227** CITATIONS
SEE PROFILE

Yixuan Yu
University of Texas at Austin
18 PUBLICATIONS **114** CITATIONS
SEE PROFILE

THE JOURNAL OF PHYSICAL CHEMISTRY Letters

Letter

pubs.acs.org/JPCL

$CuInSe_2$ Quantum Dot Solar Cells with High Open-Circuit Voltage

Matthew G. Panthani, C. Jackson Stolle, Dariya K. Reid, Dong Joon Rhee, Taylor B. Harvey, Vahid A. Akhavan, Yixuan Yu, and Brian A. Korgel*

Department of Chemical Engineering, Texas Materials Institute, and Center for Nano- and Molecular Science and Technology, The University of Texas at Austin, Austin, Texas 78712-1062, United States

Supporting Information

ABSTRACT: $CuInSe_2$ (CISe) quantum dots (QDs) were synthesized with tunable size from less than 2 to 7 nm diameter. Nanocrystals were made using a secondary phosphine selenide as the Se source, which, compared to tertiary phosphine selenide precursors, was found to provide higher product yields and smaller nanocrystals that elicit quantum confinement with a size-dependent optical gap. Photovoltaic devices fabricated from spray-cast CISe QD films exhibited large, size-dependent, open-circuit voltages, up to 849 mV for absorber films with a 1.46 eV optical gap, suggesting that midgap trapping does not dominate the performance of these CISe QD solar cells.

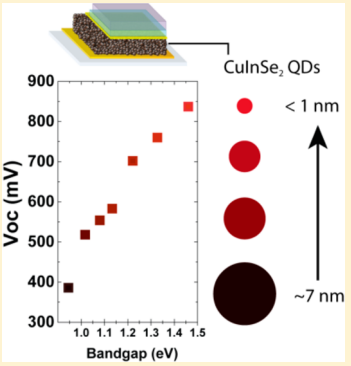

SECTION: Energy Conversion and Storage; Energy and Charge Transport

Colloidal quantum dots (QDs) are interesting materials for photovoltaic devices (PVs) due to their unique properties, like a size-tunable optical gap, enhanced absorption cross section, extended carrier lifetimes, and solution processability.[1,2] PbS and PbSe QD PVs have been made with relatively high power conversion efficiencies (PCEs) of over 7%[3,4] and high external quantum efficiency (EQE) of over 100% EQE due to multiple exciton generation, which appears to occur commonly in QDs, including Si.[5−9] A major limitation of Pb chalcogenide QD-based PVs, however, appears to be midgap carrier trapping that severely limits the open-circuit voltage.[10,11]

Higher device PCEs have been achieved by sintering nanocrystals of CdTe,[12] $Cu(In,Ga)S_2$, $Cu(In,Ga)Se_2$, and Cu_2ZnSnS_4.[13−17] Sintering, however, requires significant energy input, especially in the case of CIGS-related nanocrystals that require selenization at temperatures in excess of 500 °C, which leads to a significant increase in processing cost and complexity. Unsintered films of colloidal nanocrystals have also been explored including PbSe[3], PbS, CdSe,[18,19] and I−III−VI_2 materials such as $Cu(In_xGa_{1-x})Se_2$ (CIGS),[20] $CuIn(S,Se)_2$,[21] and Cu_2ZnSnS_4 (CZTS).[22]

A number of approaches have been developed to synthesize I−III−VI_2 nanocrystals, such as $CuInSe_2$.[16,20,23−25] One method involves reacting metal salts or complexes (such as halides, acetates, or acetylacetonates) with chalcogen powder or tertiary phosphine chalcogenides and oleylamine as a capping ligand.[16,20,23,26] Depending on the precursors or reaction conditions, this approach can yield sphalerite, chalcopyrite, or ordered-vacancy Cu−In−Se nanocrystals.[27] Wurtzite phase nanocrystals have also been made.[28] In general, this approach yields larger nonquantum confined nanocrystals with a band gap of the bulk semiconductor.

An approach to I−III−VI_2 nanocrystals that provides more size control has been the use of alkanethiols as a sulfur source and capping ligand. For example, Cu and In precursors are heated in the presence of an alkanethiol like dodecanethiol, which begins to react when heated to over 180 °C. Se can be added as a tertiary phosphine selenide. Using this approach, quantum-size $CuInS_2$ and $CuInSe_xS_{2-x}$ nanocrystals have been synthesized with size-tunable absorbance and photoluminescence and have been used for in vivo bioimaging and as sensitizers in QD-sensitized solar cells.[21,29−32]

Here, we report a new synthesis for oleylamine-capped $CuInSe_2$ (CISe) QDs. Diphenylphosphine selenide (DPP/Se) was found to be much more reactive than Se sources of tertiary phosphine selenides, trioctylphosphine selenide and tributylphosphine selenide. The use of DPP/Se in turn leads to significantly higher conversion of precursor to nanocrystals and the ability to more accurately control nanocrystal size by carrying out reactions at lower temperatures than possible using tertiary phosphine selenides. This enables the synthesis of CISe QDs without the use of thiol or S incorporation to limit the size. PV devices were made without heat or chemical treatment of the nanocrystal layer in a glass/Au/CISe QD/CdS/ZnO/ITO configuration.

Figure 1 shows TEM images of CISe QDs produced by arrested precipitation using DPP/Se reactant. (See the

Received: May 13, 2013
Accepted: May 31, 2013
Published: May 31, 2013

   dx.doi.org/10.1021/jz4010015 | J. Phys. Chem. Lett. 2013, 4, 2030−2034

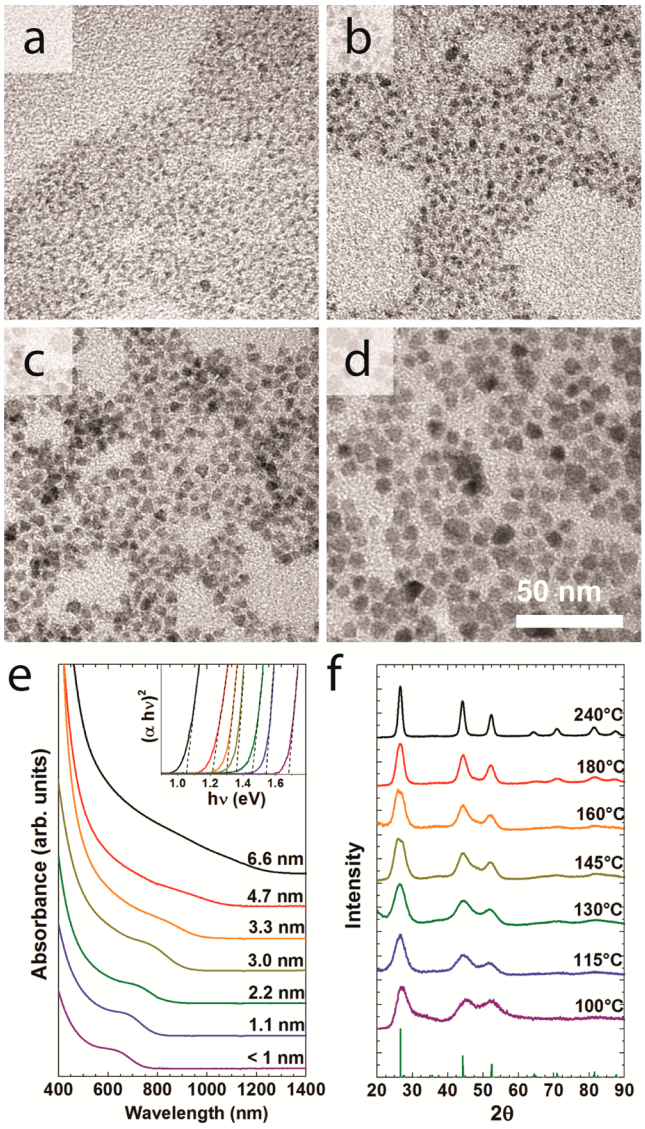

Figure 1. TEM images of CISe QDs synthesized at (a) 130, (b) 160, (c) 180, and (d) 240 °C. The average QD diameters are 2.2 ± 0.5, 3.3 ± 0.6, 4.7 ± 0.8, and 6.6 ± 1.5 nm, respectively. (e) Absorbance spectra and (f) XRD (λ = 1.54 Å) of nanocrystals synthesized at temperatures between 100 and 240 °C (<1 to 6.6 nm diameter). The inset in (e) shows Tauc plots used to determine the absorption edge reported in Table 1. The reference XRD pattern in (f) (green bars) for chalcopyrite $CuInSe_2$ is from JCPDS #97-006-8917.

Supporting Information for Experimental Details). The nanocrystal size depended on the reaction temperature, with 100 °C producing the smallest nanocrystals of diameter near 1 nm and 240 °C yielding the largest nanocrystals studied here of 6.6 ± 1.5 nm diameter. As shown in Figure 1f, X-ray diffraction (XRD) of all of the nanocrystals matched chalcopyrite $CuInSe_2$, with the expected peak broadening with decreasing nanocrystal size.

The secondary phosphine selenide reactant, DPP/Se, was found to yield significantly higher amounts of nanocrystals than the tertiary phosphine selenide, TBP/Se. Under similar reaction conditions, DPP/Se gives typical conversions of metal precursors to nanocrystals of 85% compared to only 15% when TBP/Se is used. The increase in reactant conversion using secondary phosphine selenide is similar to what has been found for PbSe nanocrystals. Evans et al.[33] for example first showed that secondary phosphine impurities in trioctylphosphine are actually the predominant reactive species in the synthesis of PbSe and CdSe nanocrystals. When they used pure DPP/Se as the Se precursor, the reaction yield was significantly higher, and the synthesis could be carried out at lower temperature than when the tertiary phosphine selenide was used. In the case of CISe QDs, the lower synthesis temperature enabled by DPP/Se enabled nanocrystals in the quantum size range to be synthesized. The Se precursor had no significant effect on the Cu/In stoichiometry. ICP-MS analysis of typical QDs synthesized with DPP/Se and TBP/Se had Cu/In ratios of 1:1.03 and 1:1.09, respectively.

The optical gap determined from absorbance spectra (Figure 1e) decreased in wavelength with decreasing size due to quantum confinement. Furthermore, nanocrystals smaller than 5 nm in diameter exhibited exciton peaks, similar to QDs of other I–III–VI_2 materials and CZTS.[21,29,30,34] The optical absorption edges of the QDs determined by extrapolation of Tauc plots (Figure 1e, inset) varied over a wide range, from 1.65 (100 °C) to 1.05 eV (240 °C); the optical gap of the largest nanocrystals was close to the bulk band gap of $CuInSe_2$ (0.95–1.05 eV).

The CISe QDs also exhibited size-dependent photoluminescence (PL) (Supporting Information, Figure S1). QDs synthesized at 100 and 115 °C exhibited PL maxima at ~735 (1.68 eV) and ~800 nm (1.55 eV), respectively. These values match the absorption edge energies determined by Tauc analysis (1.65 and 1.54 eV, respectively). Slightly larger QDs with diameters of 2–3.3 nm showed weak PL with broadened PL peaks due to the presence of some smaller diameter QDs. QDs with diameters larger than 3.3 nm showed no detectable PL between 600 and 1200 nm.

Solar cells of CISe QDs were fabricated by spray-coating under ambient conditions into a glass/Au/CISe QD/CdS/ZnO/ITO structure illustrated in Figure 2a (see the Supporting Information for device fabrication details). Figure 2b shows the current–voltage characteristics of CISe QD devices illuminated under AM1.5 (100 mW/cm^2) solar simulation. There is a trend of increasing open-circuit voltage (V_{oc}) and decreasing short-circuit current (J_{sc}) with decreasing QD diameter. Device PCEs range from 0.3 to 1.2%. Figure 2c plots the J_{sc}, V_{oc}, fill factor (FF), and PCE of devices compared to the optical gap of the CISe QDs. Relatively low J_{sc} values likely result from poor charge transport between nanocrystals due to the oleylamine capping ligands. Both FF and J_{sc} decrease with decreasing QD diameter due in part to the increasing volume fraction of oleylamine in the QD films inhibiting charge transport. There is also less light absorption as the optical gap increases, which reduces J_{sc}. V_{oc}, however, increases substantially with decreasing QD size, consistent with the larger optical gap of the nanocrystals. The highest V_{oc} observed was 849 mV, which to our knowledge is the highest reported V_{oc} obtained to date in any QD solar cell. The ratios of V_{oc} to the optical gap ($E_{g,opt}$) are higher than those of PbS and CdSe-based QD solar cells reported in the literature,[18,38] reaching as high as 76% of the theoretical maximum V_{oc} for the CISe QDs with a 1.45 eV optical gap. Figure 3 shows the ratio of the maximum theoretical open-circuit voltage calculated as described by C. H. Henry[38] to the measured open-circuit voltage of CISe QD PVs compared to those of other studies of nanocrystal PVs with high open-circuit voltage.

dx.doi.org/10.1021/jz4010015 | J. Phys. Chem. Lett. 2013, 4, 2030–2034

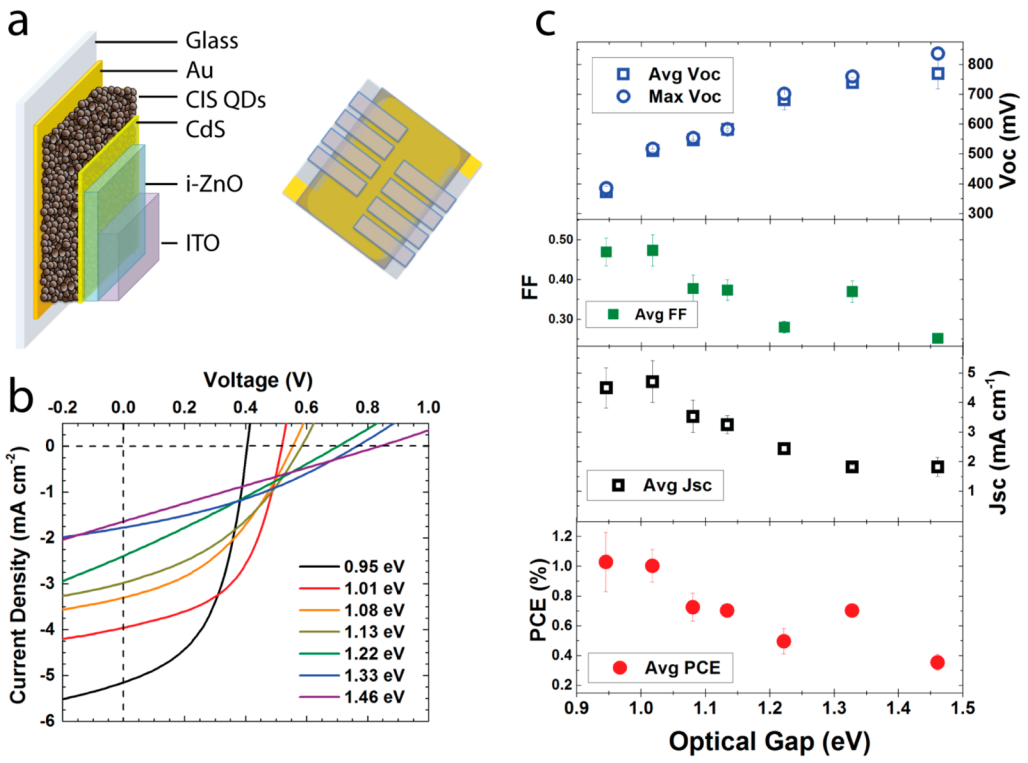

Figure 2. (A) Illustration of the cross section and top view of a CISe QD solar cell. (B) $J-V$ characteristics and (C) summary of device parameters (PCE, J_{sc}, FF, and V_{oc}) of solar cells versus the optical gap of the CISe QDs under AM1.5 illumination (100 mW/cm^2).

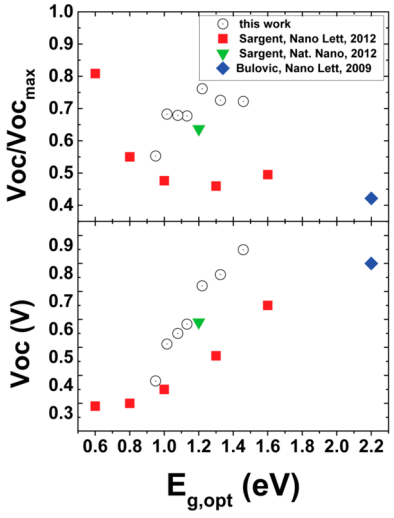

Figure 3. Fraction of the maximum theoretical open-circuit voltage (top) and reported open-circuit voltages (bottom) in this work and other works demonstrating high open-circuit voltages.[4,18,37] The theoretical maximum open-circuit voltage $V_{oc_{max}}$, is determined by the formula described by C. H. Henry.[38].

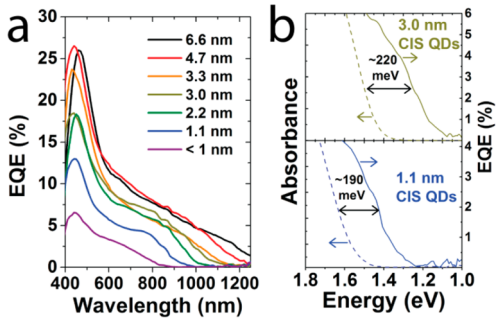

Figure 4. (a) EQE measurements of solar cells made from CISe QDs. The average QD diameter in each device is shown in the caption. (b) Comparison of the absorbance spectra of dispersed nanocrystals in toluene (dashed) and the PV EQE (solid) of 3.0 (top) and 1.1 nm (bottom) CISe QDs.

The EQE, or incident photon-to-current conversion efficiency (IPCE), was also measured for PVs made with CISe QDs of varying size. The absorption edge observed in the EQE measurements shifts systematically to lower wavelength with decreasing size, consistent with quantum confinement and the absorbance spectroscopy measurements of the solvent-dispersed QDs. Also, the EQE values generally decreased as the QD size decreased (Figure 4a), most likely from a combination of decreased absorbance with smaller size (i.e., because of the shift in absorption edge and the relatively low density of states near the band edge) and the poorer charge transport between smaller QDs. Notably though, there was a relatively large difference in energy (~200 meV) between the absorption edge observed in the EQE measurements of the devices and the absorbance spectra of the dispersions (Figure 4b). The absorption edge in the devices was significantly red-shifted in the device compared to the dispersions, as summarized in Table 1. The difference between the absorption edge observed by EQE measurements in PV devices and absorbance spectra of dispersions of PbS and PbSe QDs has been significantly smaller (~10−20 meV),[35] and usually attributed to slight differences in the dielectric environment. Red shifts of up to 120 meV have been reported in thiocyanate-capped PbSe nanocrystals annealed at 250 °C.[36] The CISe QDs, however, are not annealed or ligand-exchanged, yet there still appears to be

dx.doi.org/10.1021/jz4010015 | J. Phys. Chem. Lett. 2013, 4, 2030−2034

Table 1. Absorption Onsets of CISe QDs Determined by Absorbance Spectroscopy of Dispersions in Toluene and from EQE Measurements of PVs[a]

synthesis temperature	100 °C	115 °C	130 °C	145 °C	160 °C	180 °C	240 °C
QD diameter (nm)	<1	1.1 ± 0.4	2.2 ± 0.5	3.0 ± 0.5	3.3 ± 0.6	4.7 ± 0.8	6.6 ± 1.5
dispersion absorption edge (eV)	1.65	1.54	1.45	1.34	1.30	1.21	1.05
EQE absorption edge (eV)	1.46	1.33	1.22	1.13	1.08	1.01	0.95

[a]The nanocrystal diameter was determined by TEM.

significant electronic coupling between neighboring CISe QDs that contributes to the device response.

In summary, we show that for CISe QD synthesis, the secondary phosphine selenide precursor (DPP/Se) shows much higher reactivity compared to tertiary phosphine selenides, leading to a significant increase in product yield and the ability to react at relatively low (100−180 °C) temperatures, enabling the synthesis of nanocrystals small enough for quantum confinement and enabling the tuning of the CISe QD optical gap from 1.65 eV to about 1.0 eV. In solar cells, these QDs exhibit exceptionally high open-circuit voltages without any additional surface modification. We observe that the absorption edge in EQE measurements of solar cells has a large (~200 meV) red shift compared to the absorption edge observed in absorbance spectra of QDs dispersed in toluene, indicating that there is significant electronic coupling between QDs in the device layer. For the CISe QD solar cells, V_{oc} reached 60−75% of the theoretical maximum V_{oc}. This compares favorably to PbS QD solar cells, which to date have achieved 50−65% of the theoretical maximum V_{oc}. The high V_{oc} indicates that midgap trapping does not occur to a significant extent in these films. This is further supported by the fact that the offset between the optical gap and V_{oc} ($V_{oc} - E_{g,opt}$) is fairly insensitive to size, ranging between 0.54 and 0.64 V (Supporting Information, Figure S3). King et al.[39] argue that a constant offset between the V_{oc} and $E_{g,opt}$ signifies that carrier recombination is dominated by band-to-band processes and that trap-assisted recombination should make $V_{oc} - E_{g,opt}$ strongly dependent on the optical gap.[39] Over a similar range of $E_{g,opt}$, the PbS solar cells highlighted in Figure 3 have $V_{oc} - E_{g,opt}$ changing significantly with $E_{g,opt}$ from 0.50 V (E_g = 0.8 V) to 0.95 (E_g = 1.6 eV). Still, the CISe QDs, suffer from relatively low PCE. The low short-circuit currents are partly due to the thin absorber films that do not absorb all of the incident light but also indicate that charge transport through the film is limiting the device performance. Because these nanocrystals show high V_{oc} with low diffusion length, these QDs might be ideal for infiltration into mesoporous scaffolds, as in a QD-sensitized solar cell architecture.

■ ASSOCIATED CONTENT

Supporting Information

Experimental details, photoluminescence spectra, absorption edge determinations from EQE data, calculations of $V_{oc} - E_{g,opt}$ versus $E_{g,opt}$. This material is available free of charge via the Internet at http://pubs.acs.org.

■ AUTHOR INFORMATION

Corresponding Author

*E-mail: korgel@che.utexas.edu. Tel: +1-512-471-5633. Fax: +1-512-471-7060.

Notes

The authors declare no competing financial interest.

■ ACKNOWLEDGMENTS

Financial support of this work was provided by the Robert A. Welch Foundation (F-1464) and the National Science Foundation Industry/University Cooperative Research Center on Next Generation Photovoltaics (IIP-1134849). C.J.S. also acknowledges support for this work by the National Science Foundation Graduate Research Fellowship under Grant No. DGE-1110007.

■ REFERENCES

(1) Murray, C. B.; Norris, D. J.; Bawendi, M. G. Synthesis and Characterization of Nearly Monodisperse CdE (E = Sulfur, Selenium, Tellurium) Semiconductor Nanocrystallites. *J. Am. Chem. Soc.* **1993**, *115*, 8706−8715.

(2) Panthani, M. G.; Korgel, B. A. Nanocrystals for Electronics. *Ann. Rev. Chem. Biomol. Eng.* **2012**, *3*, 287−311.

(3) Luther, J. M.; Law, M.; Beard, M. C.; Song, Q.; Reese, M. O.; Ellingson, R. J.; Nozik, A. J. Schottky Solar Cells Based on Colloidal Nanocrystal Films. *Nano Lett.* **2008**, *8*, 3488−3492.

(4) Ip, A. H.; Thon, S. M.; Hoogland, S.; Voznyy, O.; Zhitomirsky, D.; Debnath, R.; Levina, L.; Rollny, L. R.; Carey, G. H.; Fischer, A.; et al. Hybrid Passivated Colloidal Quantum Dot Solids. *Nat. Nanotechnol.* **2012**, *7*, 577−582.

(5) Semonin, O. E.; Luther, J. M.; Choi, S.; Chen, H.-Y.; Gao, J.; Nozik, A. J.; Beard, M. C. Peak External Photocurrent Quantum Efficiency Exceeding 100% via MEG in a Quantum Dot Solar Cell. *Science* **2011**, *334*, 1530−1533.

(6) Ellingson, R. J.; Beard, M. C.; Johnson, J. C.; Yu, P.; Micic, O. I.; Nozik, A. J.; Shabaev, A.; Efros, A. L. Highly Efficient Multiple Exciton Generation in Colloidal PbSe and PbS Quantum Dots. *Nano Lett.* **2005**, *5*, 865−871.

(7) Murphy, J. E.; Beard, M. C.; Norman, A. G.; Ahrenkiel, S. P.; Johnson, J. C.; Yu, P.; Micic, O. I.; Ellingson, R. J.; Nozik, A. J. PbTe Colloidal Nanocrystals: Synthesis, Characterization, and Multiple Exciton Generation. *J. Am. Chem. Soc.* **2006**, *128*, 3241−3247.

(8) Luther, J. M.; Beard, M. C.; Song, Q.; Law, M.; Ellingson, R. J.; Nozik, A. J. Multiple Exciton Generation in Films of Electronically Coupled PbSe Quantum Dots. *Nano Lett.* **2007**, *7*, 1779−1784.

(9) Beard, M. C.; Knutsen, K. P.; Yu, P.; Luther, J. M.; Song, Q.; Metzger, W. K.; Ellingson, R. J.; Nozik, A. J. Multiple Exciton Generation in Colloidal Silicon Nanocrystals. *Nano Lett.* **2007**, *7*, 2506−2512.

(10) Tang, J.; Brzozowski, L.; Barkhouse, D. A.; Wang, X.; Debnath, R.; Wolowiec, R.; Palmiano, E.; Levina, L.; Pattantyus-Abraham, A. G.; Jamakosmanovic, D.; et al. Quantum Dot Photovoltaics in the Extreme Quantum Confinement Regime: The Surface-Chemical Origins of Exceptional Air- and Light-Stability. *ACS Nano* **2010**, *4*, 869−878.

(11) Nagpal, P.; Klimov, V. I. Role of Mid-Gap States in Charge Transport and Photoconductivity in Semiconductor Nanocrystal Films. *Nat. Commun.* **2011**, *2*, 486.

(12) Jasieniak, J.; MacDonald, B. I.; Watkins, S. E.; Mulvaney, P. Solution-Processed Sintered Nanocrystal Solar Cells via Layer-by-Layer Assembly. *Nano Lett.* **2011**, *11*, 2856−2864.

(13) Guo, Q.; Ford, G. M.; Yang, W.-C.; Walker, B. C.; Stach, E. A.; Hillhouse, H. W.; Agrawal, R. Fabrication of 7.2% Efficient CZTSSe Solar Cells Using CZTS Nanocrystals. *J. Am. Chem. Soc.* **2010**, *132*, 17384−17386.

(14) Guo, Q.; Ford, G. M.; Hillhouse, H. W.; Agrawal, R. Sulfide Nanocrystal Inks for Dense $Cu(In_{1-x}Ga_x)(S_{1-y}Se_y)_2$ Absorber Films and Their Photovoltaic Performance. *Nano Lett.* **2009**, *9*, 3060−3065.
(15) Guo, Q.; Hillhouse, H. W.; Agrawal, R. Synthesis of Cu_2ZnSnS_4 Nanocrystal Ink and Its Use for Solar Cells. *J. Am. Chem. Soc.* **2009**, *131*, 11672−11673.
(16) Guo, Q.; Kim, S. J.; Kar, M.; Shafarman, W. N.; Birkmire, R. W.; Stach, E. A.; Agrawal, R.; Hillhouse, H. W. Development of $CuInSe_2$ Nanocrystal and Nanoring Inks for Low-Cost Solar Cells. *Nano Lett.* **2008**, *8*, 2982−2987.
(17) Akhavan, V. A.; Harvey, T. B.; Stolle, C. J.; Ostrowski, D. P.; Glaz, M. S.; Goodfellow, B. W.; Panthani, M. G.; Reid, D. K.; Vanden Bout, D. A.; Korgel, B. A. Influence of Composition on the Performance of Sintered $Cu(In,Ga)Se_2$ Nanocrystal Thin-Film Photovoltaic Devices. *ChemSusChem* **2013**, *6*, 481−486.
(18) Arango, A. C.; Oertel, D. C.; Xu, Y.; Bawendi, M. G.; Bulovic, V. Heterojunction Photovoltaics using Printed Colloidal Quantum Dots as a Photosensitive Layer. *Nano Lett.* **2009**, *9*, 860−863.
(19) Robel, I.; Subramanian, V.; Kuno, M.; Kamat, P. V. Quantum Dot Solar Cells. Harvesting Light Energy with CdSe Nanocrystals Molecularly Linked to Mesoscopic TiO_2 Films. *J. Am. Chem. Soc.* **2006**, *128*, 2385−2393.
(20) Panthani, M. G.; Akhavan, V.; Goodfellow, B.; Schmidtke, J. P.; Dunn, L.; Dodabalapur, A.; Barbara, P. F.; Korgel, B. A. Synthesis of $CuInS_2$, $CuInSe_2$, and $Cu(In_xGa_{1-x})Se_2$ (CIGS) Nanocrystal "Inks" for Printable Photovoltaics. *J. Am. Chem. Soc.* **2008**, *130*, 16770−16777.
(21) McDaniel, H.; Fuke, N.; Pietryga, J. M.; Klimov, V. I. Engineered $CuInSe_xS_{2-x}$ Quantum Dots for Sensitized Solar Cells. *J. Phys. Chem. Lett.* **2013**, *4*, 355−361.
(22) Steinhagen, C.; Panthani, M. G.; Akhavan, V.; Goodfellow, B.; Koo, B.; Korgel, B. A. Synthesis of Cu_2ZnSnS_4 Nanocrystals for Use in Low-Cost Photovoltaics. *J. Am. Chem. Soc.* **2009**, *131*, 12554−12555.
(23) Akhavan, V. A.; Goodfellow, B. W.; Panthani, M. G.; Reid, D. K.; Hellebusch, D. J.; Adachi, T.; Korgel, B. A. Spray-Deposited $CuInSe_2$ Nanocrystal Photovoltaics. *Energy Environ. Sci.* **2010**, *3*, 1600−1606.
(24) Koo, B.; Patel, R. N.; Korgel, B. A. Synthesis of $CuInSe_2$ Nanocrystals with Trigonal Pyramidal Shape. *J. Am. Chem. Soc.* **2009**, *131*, 3134−3135.
(25) Zhong, H.; Wang, Z.; Bovero, E.; Lu, Z.; van Veggel, F. C. J. M.; Scholes, G. D. Colloidal $CuInSe_2$ Nanocrystals in the Quantum Confinement Regime: Synthesis, Optical Properties, and Electroluminescence. *J. Phys. Chem. C* **2011**, *115*, 12396−12402.
(26) Akhavan, V. A.; Panthani, M. G.; Goodfellow, B. W.; Reid, D. K.; Korgel, B. A. Thickness-Limited Performance of $CuInSe_2$ Nanocrystal Photovoltaic Devices. *Opt. Express* **2010**, *18*, A411−A420.
(27) Allen, P. M.; Bawendi, M. G. Ternary I−III−VI Quantum Dots Luminescent in the Red to Near-Infrared. *J. Am. Chem. Soc.* **2008**, *130*, 9240−9241.
(28) Koo, B.; Patel, R. N.; Korgel, B. A. Wurtzite-Chalcopyrite Polytypism in $CuInS_2$ Nanodisks. *Chem. Mater.* **2009**, *21*, 1962−1966.
(29) Cassette, E.; Pons, T.; Bouet, C.; Helle, M.; Bezdetnaya, L.; Marchal, F.; Dubertret, B. Synthesis and Characterization of Near-Infrared Cu−In−Se/ZnS Core/Shell Quantum Dots for In Vivo Imaging. *Chem. Mater.* **2010**, *22*, 6117−6124.
(30) Pons, T.; Pic, E.; Lequeux, N.; Cassette, E.; Bezdetnaya, L.; Guillemin, F.; Marchal, F.; Dubertret, B. Cadmium-Free $CuInS_2$/ZnS Quantum Dots for Sentinel Lymph Node Imaging with Reduced Toxicity. *ACS Nano* **2010**, *4*, 2531−2538.
(31) Li, L.; Pandey, A.; Werder, D. J.; Khanal, B. P.; Pietryga, J. M.; Klimov, V. I. Efficient Synthesis of Highly Luminescent Copper Indium Sulfide-Based Core/Shell Nanocrystals with Surprisingly Long-Lived Emission. *J. Am. Chem. Soc.* **2011**, *133*, 1176−1179.
(32) Santra, P. K.; Nair, P. V.; George Thomas, K.; Kamat, P. V. $CuInS_2$-Sensitized Quantum Dot Solar Cell. Electrophoretic Deposition, Excited-State Dynamics, and Photovoltaic Performance. *J.Phys. Chem. Lett.* **2013**, *4*, 722−729.
(33) Evans, C. M.; Evans, M. E.; Krauss, T. D. Mysteries of TOPSe Revealed: Insights into Quantum Dot Nucleation. *J. Am. Chem. Soc.* **2010**, *132*, 10973−10975.
(34) Khare, A.; Wills, A. W.; Ammerman, L. M.; Norris, D. J.; Aydil, E. S. Size Control and Quantum Confinement in Cu_2ZnSnS_4 Nanocrystals. *Chem Commun.* **2011**, *47*, 11721−11723.
(35) Law, M.; Beard, M. C.; Choi, S.; Luther, J. M.; Hanna, M. C.; Nozik, A. J. Determining the Internal Quantum Efficiency of PbSe Nanocrystal Solar Cells with the Aid of an Optical Model. *Nano Lett.* **2008**, *8*, 3904−3910.
(36) Choi, J. H.; Fafarman, A. T.; Oh, S. J.; Ko, D. K.; Kim, D. K.; Diroll, B. T.; Muramoto, S.; Gillen, J. G.; Murray, C. B.; Kagan, C. R. Bandlike Transport in Strongly Coupled and Doped Quantum Dot Solids: A Route to High-Performance Thin-Film Electronics. *Nano Lett.* **2012**, *12*, 2631−2638.
(37) Tang, J.; Liu, H.; Zhitomirsky, D.; Hoogland, S.; Wang, X.; Furukawa, M.; Levina, L.; Sargent, E. H. Quantum Junction Solar Cells. *Nano Lett.* **2012**, *12*, 4889−4894.
(38) Henry, C. H. Limiting Efficiencies of Ideal Single and Multiple Energy Gap Terrestrial Solar Cells. *J. Appl. Phys.* **1980**, *51*, 4494−4500.
(39) King, R. R.; Bhusari, D.; Boca, A.; Larrabee, D.; Liu, X. Q.; Hong, W.; Fetzer, C. M.; Law, D. C.; Karam, N. H. Band Gap-Voltage Offset and Energy Production in Next-Generation Multijunction Solar Cells. *Prog. Photovolt. Res. Appl.* **2011**, *19*, 797−812.